XLIII CILAMCE
21–25, November, 2022
FOZ DO IGUAÇU – PR – BRAZIL

Analytical and numerical comparison of bearing capacity of strip foundation on slopes

Marko López[1], Anthony Flores[1], Saskia Arévalo[1]

[1]*Civil Engineering Department, Universidad de Lima, Lima, Perú*
Av. Javier Prado Este 4600, Santiago de Surco, 15023, Lima, Perú
mlopezb@ulima.edu.pe, 20172129@aloe.ulima.edu.pe, 20172844@aloe.ulima.edu.pe

Abstract. Several engineering projects such as buildings, transmission towers and bridge abutments are founded in areas adjacent to a slope. When this occurs, the behavior of the foundation is affected by presence of the slope, which modifies its bearing capacity and failure mechanism of the ground, being substantially different from that developed by footings on horizontal geomorphologies. In 1957, Meyerhof was a pioneer in developing a theory to determine the bearing capacity of a foundation in areas adjacent to a slope, and his work was complemented by several researchers in later years and is still under study today. This paper presents a comparison of the available methods developed by different authors to estimate the bearing capacity of a strip footing at the top of the slope. In addition, the calculation of the bearing capacity is determined using the finite element method with the Abaqus program. Finally, a parametric numerical study is carried out on the effects of slope height, distance to the footing crest/width and soil strength parameters and slope angle are found to be the most influential. In the end it is concluded that the analytical solutions have limitations, and the numerical model turns out to be faster and the changes can be better appreciated.

Keywords: bearing capacity, finite element analysis, slopes, strip footings.

1 Introduction

Foundations are a fundamental pillar for any structure, as they transmit the load from the superstructure to the ground. Due to various situations such as space constraints, economic, geomorphological and architectural objectives in a project, there is a need to build close to a slope. When a foundation is built on a slope, one side of the foundation will be subjected to the slope and plastic regions will be developed, producing significant changes in slope stability, and bearing capacity of the foundation. Bearing capacity is an important concern in geotechnics, especially when analyzing and determining the capacity of the foundation near a slope. The first theories regarding the bearing capacity of soils were studied by Terzaghi (1943) allowing other authors to continue the research such as Meyerhof (1957), Hansen (1970), Vesic (1975), Graham (1988), Saran et al. (1989), Sarma and Chen (1995), Georgiadis (2010) or Shiau (2011).

Meyerhof (1957) investigated the failure mechanism and bearing capacity of foundations in cohesive and granular soils adjacent to slopes. For this method, the bearing capacity factors N_{cq} and $N_{\gamma q}$ are available, which depend on a stability factor N_s as a function of slope inclination (β) and distance to the slope edge; these can be obtained from simplified abacuses. Then, Hansen (1970) and Vesic (1975), evaluated the bearing capacity for a foundation that is located on the crest of a slope. The authors incorporated parameters such as depth factor, slope angle and soil weight in their analysis for the bearing capacity for undrained conditions, managing to establish the value of the load factor N_c as negative. Both solutions are applicable for footings on a slope or on the crest of a slope and when the load is inclined towards the slope. Graham (1988) provided a solution for the load capacity factor for a shallow continuous foundation at the top of a slope from the relationships between the depth of the foundation (D_f), width of the foundation (B), and the distance to the crest (b). Saran et al. (1989) provided a solution to obtain the bearing capacity of the foundation adjacent to slopes from limit equilibrium analysis considering the unilateral failure and the angle of internal friction along the slope, using a set of dimensionless plots. Sarma and Chen (1995) used the limit equilibrium method to estimate the seismic bearing capacity factors for footings

considering values from trial and error. Similarly, they present their analysis in a table comparing values of internal friction angle and slope angle coefficients.

In the next decade Georgiadis (2010) investigated the influence of inclined loading on the failure mechanism. Finite element, upper bound plasticity and stress field methods were used to examine a wide range of geometries and soil properties that affect the value of the bearing capacity of slope foundations in undrained soils. In turn, Shiau et al. (2011) used the finite element analysis method making use of dimensionless parameters to obtain the top and bottom of the bearing capacity value of foundations on a slope in cohesive soils. The aforementioned authors extended their analysis from Meyerhof's proposal for this type of situation, of shallow foundations on the crest of a slope.

Likewise, present investigation has compiled analytical solutions for estimating the slope bearing capacity of the aforementioned authors and is described in Table 1.

Table 1: Ultimate bearing capacity equations.

Author	Year	Equation	Factors
Meyerhof	1957	$q_u = cN_{cq} + \frac{1}{2}\gamma B N_{\gamma q}$	$N_{\gamma q}, N_{cq}$
Hansen	1970	$q_u = cN_c\lambda_{c\beta} + qN_q\lambda_{q\beta} + \frac{1}{2}\gamma B N_\gamma \lambda_{\gamma\beta}$	$N_q = e^{\pi tantan\,\phi}\left(\frac{1+sin\,sin\,\phi}{1-sin\,sin\,\phi}\right)$ $N_c = (N_q - 1)\,cot\,cot\,\phi$ $N_\gamma = 1.5N_c\phi$ $\lambda_{q\beta} = \lambda_{\gamma\beta} = (1 - tan\,tan\,\beta\,)^2$ $\lambda_{c\beta} = \frac{N_q\lambda_{q\beta} - 1}{N_q - 1}$
Vesic	1975	$q_u = (5.14 - 2\beta)c + \gamma D_f(1 - tan\,tan\,\beta\,)^2 - \gamma B\, sin\,\sin\beta\,(1 - tan\,\tan\beta)^2$	$N_\gamma = -2\,sin\,sin\,\beta$
Graham	1988	$q_u = \frac{1}{2}\gamma B N_{\gamma q}$	$N_{\gamma q}$ *from plots based on* $(\frac{D_f}{B})$ *and* $(\frac{b}{B})$
Saran et al.	1989	$q_u = cN_c + qN_q + \frac{1}{2}\gamma B N_\gamma$	N_c, N_q, N_γ *obtained from graphics*
Sarma and Chen	1995	$q_u = cN_c + qN_q + 0.5\gamma B N_\gamma$	$log\,log\,(N_c) = a\beta^2 + b\beta + c$ $log\,log\,(N_q) = \beta + b\ tan\,tan\,\beta + c$ $log\,log\,(N_\gamma) = \beta + b\ tan\,tan\,\beta + c$
Georgiadis	2010	$q_u = C_u N_c$	$N_{Co} = 5.14 - \frac{2\beta}{1 - \frac{\gamma\beta}{5.14C_u}}$ $N_c = N_{Co} + (5.14 - N_{Co})\frac{\lambda}{\lambda_o}\left[1 + \frac{\beta}{2}\left(1 - \frac{\lambda}{\lambda_0}\right)\right]$ $\lambda_o = \left(\frac{5.14}{2}\right)^\beta, \lambda = \frac{b}{B}$
Shiau et al.	2011	$Without\ exact\ solution$	$\frac{p}{\gamma B} = f\left(\beta, \frac{L}{B}, \frac{C_u}{\gamma B}, \frac{q}{\gamma B}, \frac{H}{B}\right)$

Then, a 2D numerical model for a spread footing on the crest of a slope was performed using finite element software (Abaqus, 2021). In the simulations, initial conditions of the soil, such as its stresses, are defined as a function of its depth and specific weight, the soil is considered the Mohr-Coulomb elastoplastic constitutive model to determine and analyze its impact on both the bearing capacity and settlement of the footing.

The present study constitutes an approach to the evaluation of the failure mechanism and the determination of the bearing capacity of shallow foundations running on the crest of a slope through analytical solutions and numerical simulation. The results obtained highlight the importance of the correct evaluation of the bearing capacity and the use of the numerical model for its calibration, later to perform more advanced numerical analyses.

2 Analytics Solutions

The present paper has focused on the evaluation of the bearing capacity on a 2D model of a foundation supported on the top of the slope (see Fig. 1), where: *B* is the foundation width, *b* is the distance from the foundation edge to the slope crest, D_f is the foundation depth, *H* is the slope height and β is the slope inclination angle.

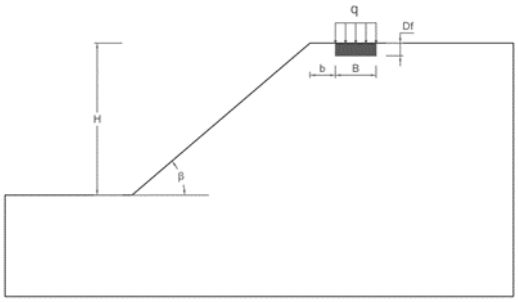

Figure 1: Description of the model and geometric parameters evaluated.

The evaluation of the analytical solutions has prioritized the use of the solutions proposed by Vesic (1975) and Georgiadis (2010), for purely cohesive soils, and by Hansen (1970) and Sarma and Chen (1995) for cohesive-frictional soils. Likewise, the evaluation consisted of modifying the various evaluation parameters (D_f/B, b, H and β) and evaluating the bearing capacity results. For the estimation of the ultimate capacity a study has been carried out which has consisted of modifying the various geometric parameters, these are, D_f/B, b, H and β. For all analyses it is considered that the footing width is 2 m, the slope height is 8 m; with four levels of closeness to the slope of b/B = 0.1, 0.5, 1 and 2; four depth conditions D_f/B = 0, 0.5, 1, 2 and three levels of slope inclination β = 15°, 30° and 45°. The soil specific gravity is 18 kN/m^3 for all cases analyzed. For a cohesive soil (Case I) and frictional soils (Case II). For cohesive soils the analytical proposals of Vesic (1975) and Georgiadis (2010) are used, and the undrained cohesion value is variable where c_u = 60, 90 and 120 kPa. For the case of frictional soils, the analytical expressions of Hansen (1970) and Sarma and Chen (1995) are used, and the friction angles evaluated present the values of ϕ = 20°, 30° and 40°. Finally, the bearing capacity failure modes of a slope foundation, where the general failure mode is omitted, are evaluated according to modes (a) and (b) described in Fig. 2.

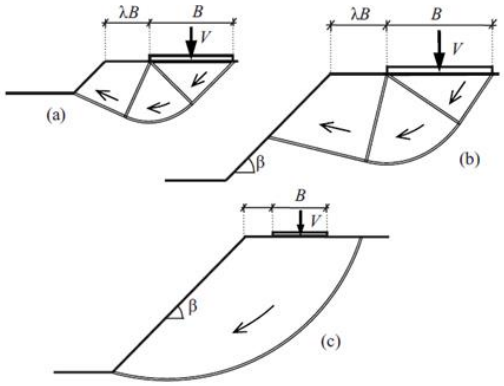

Figure 2: Failure modes by bearing capacity (a and b) and by general slope failure (c) (Georgiadis, 2010).

3 Numerical Model

In this part, the finite element-based software Abaqus (2021), which works with effective finite element-based stresses, was used in the plane state of deformation to calculate the bearing capacity of a rigid strip footing located on a slope under a vertical load. Fig. 3 presents the description of the geometric parameters and mesh of the model. To eliminate the effects of contours due to loading, the horizontal and vertical contours must be located at an adequate distance from the foundation. In this study, a sensitivity analysis on the influence of contours was not performed and the parameter description presented was found to be appropriate as other researchers (Ahmadi and Asakereh, 2015). The soil is modeled by quadrilateral solid elements adopt linear interpolation for displacements (CPE4), the sensitivity of using elements with quadratic interpolation (CPE8) was not performed. In total, the mesh has 2739 elements with 4-point Gaussian integration and 2838 nodes. Due to stress concentration around the foundation, the mesh size was locally refined in this region. With respect to the boundary conditions, the horizontal displacements are constrained on the right and left sides; and at the bottom of the model, horizontal and vertical displacements are restricted.

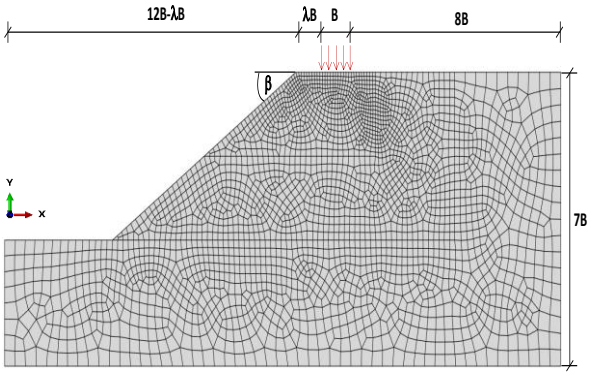

Figure 3: Model and mesh for numerical analysis.

For its simplicity, mechanical behavior of soil is represented through the Mohr-Coulomb (MC) elastic-plastic constitutive model, where the yield surface is generally given by a shear failure function based on the frictional character of soils. MC does not take into account the occurrence of plastic deformations due to the application of hydrostatic loads. On the other hand, critical state models are able to better represent this behavior, such as the "Cap models" (Sandler et al., 1976; Resende et al., 1985, López and Quevedo, 2022). The MC model requires five input parameters, for this study we adopted: Young's modulus of elasticity (E=30600kPa), Poisson's coefficient (ν=0.2), φ denotes the slope of the Mohr-Coulomb yield surface in the meridional stress plane (φ=20°), cohesion (c=60kPa), dilatation angle (ψ=φ) and as a parameter of the overall numerical model is the specific gravity (γ=18kN/m^3). As in previous studies (Lee and Salgado, 2005; Mabrouki et al., 2010; Baazouzi et al., 2016), it was observed that the values of Young's modulus and Poisson's ratio affect the evolution of footing settlement but do not affect the value of collapse load.

During the displacement-controlled finite element analysis, it was applied in the following steps: i) geostatic equilibrium; ii) gravity throughout the model; and iii) vertical displacement applied on the footing incrementally from zero until the ultimate load was reached.

The first step, the initial geostatic stresses must be in equilibrium with the applied loads and boundary conditions. Ideally, the vertical and horizontal stresses ($\sigma'_h=K_0\cdot\sigma'_v$, where K_0=0.5) should balance exactly and produce zero deformations. This state is obtained by performing an initial analysis in Abaqus, fixing all the degrees of freedom of the displacements. Fig. 4a shows the initial geostatic stresses. Then, in the second step of the analysis, the calculated reaction forces are used to create nodal point forces and the displacement degrees of freedom are released from the model, where the geostatic stress field of the slope is obtained as shown in Fig. 4b and it is observed that the vertical stresses at the ground level and on the slope vary incrementally as expected before proceeding to apply the load. Finally, an incremental vertical displacement up to 10% of the footing width is applied to all nodes at the soil-slab interface. This condition is imposed to represent the settlement of a rigid foundation.

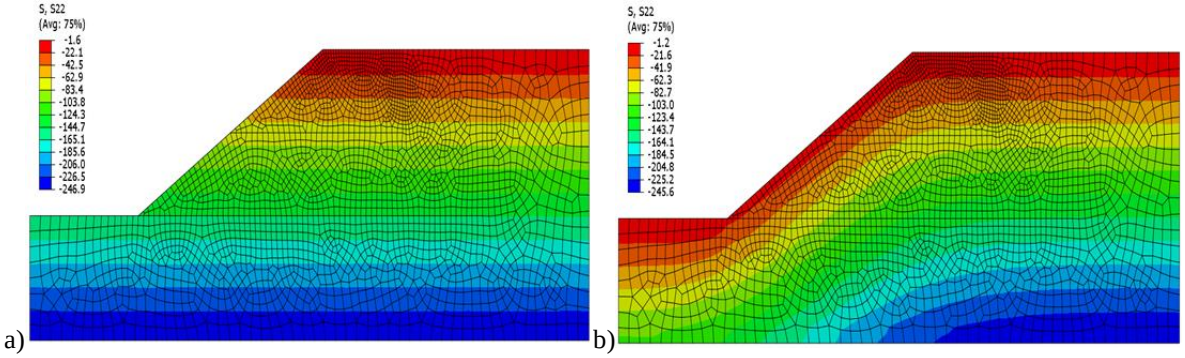

a) b)

Figure 4: Vertical effective stress: a) initial step and b) after applying gravity and equilibrium.

4 Results and discussion

4.1 Case I: cohesive soil

Fig. 5a presents the bearing capacity as a function of the incidence of slope inclination angle (β) and

undrained cohesion (c_u) results of the solutions of Vesic (1975) and Georgiadis (2010). Both expressions show a continuous decrease in their ultimate capacity results as the slope inclination angle increases, but their proposals present differences where the proposal of Vesic (1975) doubles the value obtained by Georgiadis (2010), as shown in Fig. 5b, with this relationship tending to reach the value of 2.24 when the slope inclination angle increases, in none of the cases this relationship was lower than 2.05.

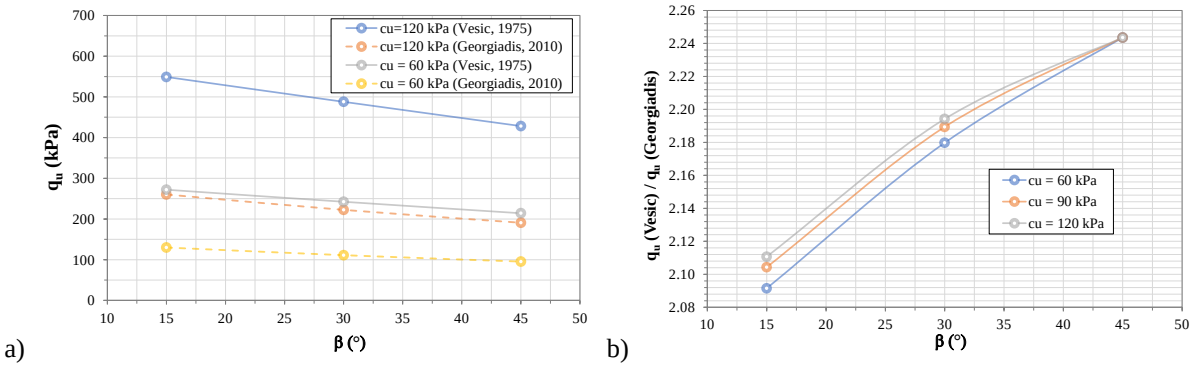

a) b)

Figure 5: Bearing capacity at the slope crest for cohesive soils for c_u = 60-120 kPa and β=15-45°.

In Fig. 6a the incidence of the distance to the slope crest is presented. Vesic's expression (1975) does not take this factor into account and, therefore, shows constant bearing capacity results of 544, 485 and 428 kPa for any *b*/*B* ratio and for slope inclination angles (β) of 15 , 30 and 45°, respectively. The expression of Georgiadis (2010) includes this influence in its expression and presents descending values with the proximity to the crest of the slope. Likewise, Fig. 6b presents the incidence of the evaluation of the influence of depth (D_f/B) on the ultimate capacity, which shows that there is low sensitivity to this variation in the Vesic expression, approximately 14%, and no incidence in the Georgiadis expression.

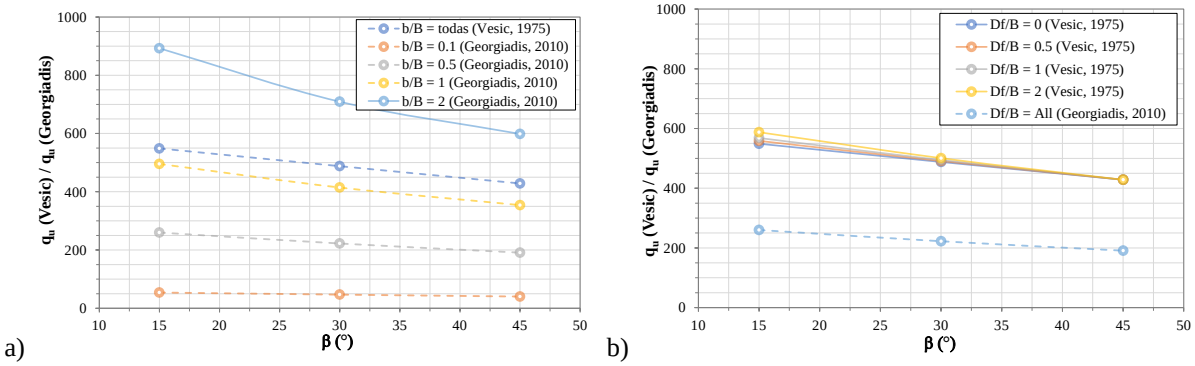

a) b)

Figure 6: Bearing capacity at the slope crest for cohesive soils: a) *b*/*B* and b) D_f/B.

4.2 Case II: friction soil

Fig. 7a presents the bearing capacity as a function of slope inclination angle (β) and internal friction angle (ϕ) results evaluated with the expressions of Hansen (1970) and Sharma and Chen (1995). Both expressions show a continuous decrease in their ultimate capacity results as the slope inclination angle increases, but their proposals present differences where the proposal of Sharma and Chen (1970) doubles the value obtained by Hansen (1995), as shown in Fig. 7b, having this relationship at an average value of 2.16 and with a tendency to increase as the value of β increases, reaching a value of 2.46 and 3.91 for friction angles of 30° and 40°, respectively.

Fig. 8 shows the bearing capacity with respect to the incidence of the distance to the slope crest, evaluated for a slope inclination angle (β) of 15°, 30° and 40°. The expressions of Hansen (1970) and Sharma and Chen (1995) do not take into account this factor (*b*/*B*) and, therefore, evidence constant results for any of their relationships. However, a continuous decrease in bearing capacity is observed with increasing slope inclination angle (β).

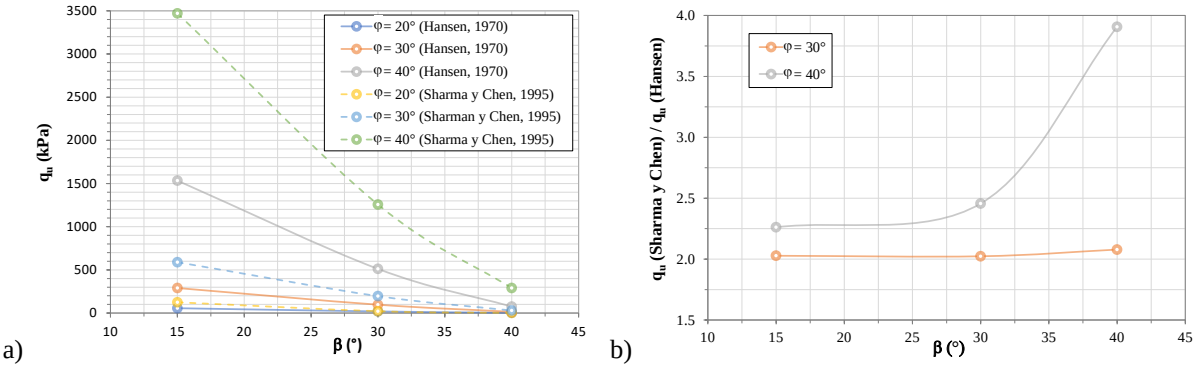

a) b)

Figure 7: Bearing capacity at the slope crest for frictional soils φ=20- 40° and β=15- 45°.

Fig. 9a presents the bearing capacity with respect to the incidence of foundation depth (D_f/B) if it is considered in both expressions, showing values of allowable capacity in the proposals of Sharma and Chen (1995). In both cases, the value of the bearing capacity decreases with the increase of the slope inclination angle and increases with the deepening of the foundation. The relationship between ultimate soil capacities by the analytical methods of Sharma and Chen and Hansen, as presented in Fig. 9b, evidences a relationship of between 1.40, for β=15°, and 4.38, for β = 40°.

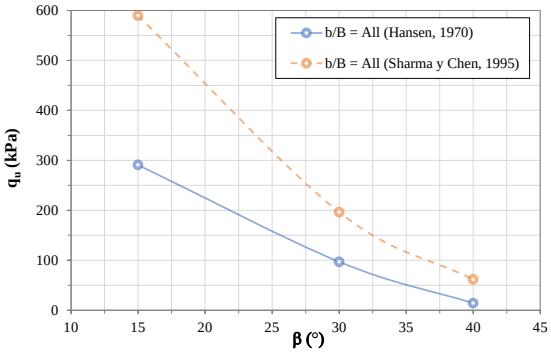

Figure 8: Bearing capacity at slope crest for frictional soils near slope *b*/*B*.

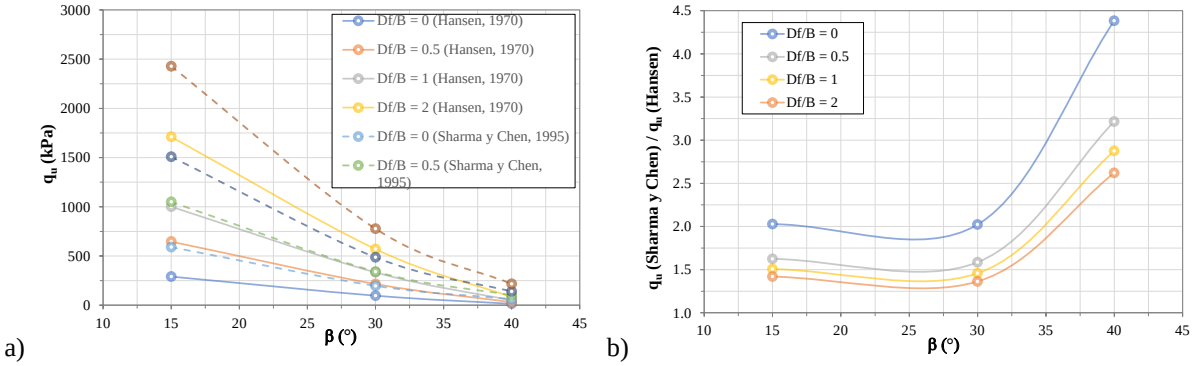

a) b)

Figure 9: Bearing capacity at the slope crest for cohesive soils as a function of D_f/B and β=15- 45°.

The simulations are performed assuming drained conditions (Δu_w=0 kPa), whereby the finite element results obtained from a footing 2 m wide (*b*/*B*=1) on a slope with a height of 8 m, and an inclination of 30° and with the soil properties explained in item 3 of the article are presented. In the load versus settlement curves in Fig. 10, for case I, varying c = 60, 90 and 120 kPa and with the slope angle increasing (β = 15°, 30° and 45°). It can be observed that the resulting curves are typical of not so stiff soils with close values between variations; in Fig. 11, for case II in stiff soils presenting friction angle (φ) the curve develops sharp increases of settlement after reaching the maximum bearing capacity of which the variations are observed for each increase of friction and cohesion. In other numerical studies, the ultimate bearing capacity was considered equal to the pressure at a settlement of 10% of the footing width, unless the maximum pressure is observed before this settlement (Ahmadi and Asakereh, 2015).

As can be seen in the results obtained, load-settlement curves in Fig. 10 show the bearing capacity obtained

at 10% of the footing width of 2m. For the first case shown, it can be observed that as the cohesion increases, the bearing capacity will also increase, but if the angle of inclination is increased, it can be observed that there is a decrease in the bearing capacity. In Fig. 11, second case is seen for an inclination angle of $\beta = 30°$ but with different friction angle (φ), as the cohesion increases also increases the bearing capacity, but at the same time if the friction angle is increased it is observed that it maintains the same behavior of increase in the bearing capacity, those results can be better appreciated in Table 2 that makes comparisons with the results obtained from the analytical solutions and the behavior of it.

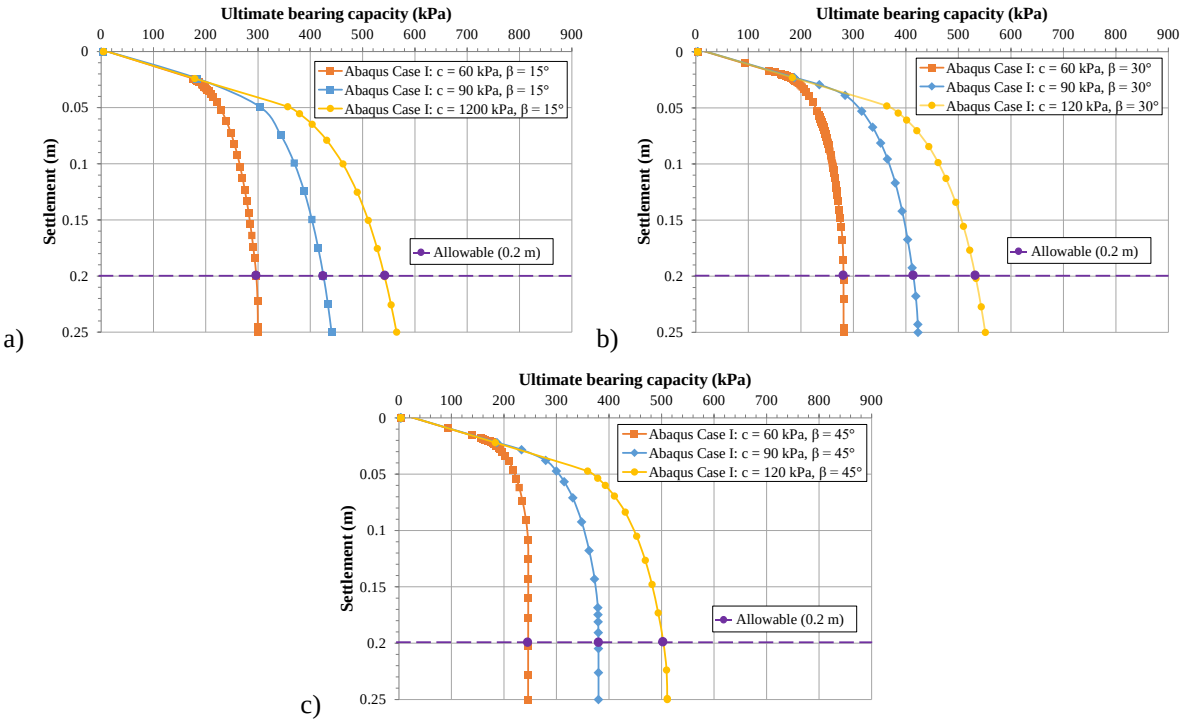

Figure 10: Load-settlement curve under the footing (Abaqus Case I).

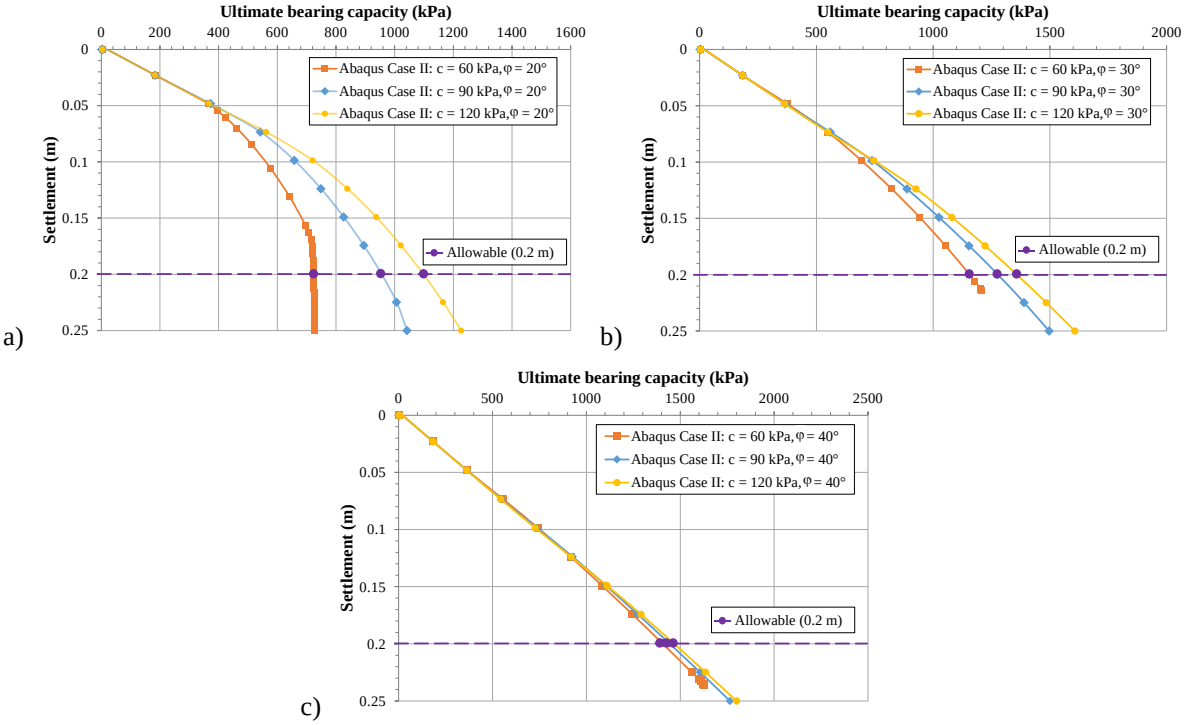

Figure 11: Load-settlement curve under the footing (Abaqus Case II).

Likewise, comparisons of the results of the bearing capacity by analytical methods and of the numerical model are made, dividing them into their respective cases (Case I and Case II) and are described in Table 2. As can be seen in Table 2; the results of the finite element method (FEM), Abaqus Case I, and referring to the analytical results between the authors Vesic and Georgiadis, it can be seen that as the cohesion increases, the bearing capacity will also increase, but if the slope inclination increases, the bearing capacity decreases but with the same behavior already mentioned.

For the results of Abaqus Case II, that contemplates the friction angle and referring to the analytical results between the authors Hansen and Sarma & Chen, it can be observed that as the cohesion increases the bearing capacity will increase, but if the friction angle is increased at the same slope inclination, it is observed that the bearing capacity has an ascending behavior according to the increase of the cohesion and the friction angle. It can be seen that they conserve the same behavior as cohesion increases in both cases, the main difference is when the slope friction is increased, which generates significant increases in the bearing capacity.

Table 2: Summary of bearing capacity (kPa) results.

		FEM	**Vesic**	**Georgiadis**
Abaqus Case I		β = 15° and φ = 0°		
	Cu = 60	296.6764088	271.990848	247.779913
	Cu = 90	425.2542665	410.482885	371.669869
	Cu = 120	541.9468413	548.974921	495.559825
		FEM	**Vesic**	**Georgiadis**
		β = 30° and φ = 0°		
	Cu = 60	281.0527139	242.352757	207.343909
	Cu = 90	413.9134972	365.1368	311.015864
	Cu = 120	532.5014673	487.9209	414.687819
		FEM	**Vesic**	**Georgiadis**
		β = 45° and φ = 0°		
	Cu = 60	246.048918	214.152	177.154675
	Cu = 90	379.7651171	321.228	265.732012
	Cu = 120	503.7708264	428.309	354.30935
		FEM	**Hansen**	**Sarma & Chen**
Abaqus Case II		β = 30° and φ = 20°		
	Cu = 60	723.6315585	33.0751076	44.8293987
	Cu = 90	955.7968172	44.8734529	63.5006765
	Cu = 120	1097.942565	56.6717983	82.1719542
		β = 30° and φ = 30°		
	Cu = 60	1156.07775	286.131907	377.830058
	Cu = 90	1277.120479	404.970193	530.439773
	Cu = 120	1358.503636	523.80848	683.049488
		β = 30° and φ = 40°		
	Cu = 60	1407.318589	1004.2256	2372.22572
	Cu = 90	1444.40785	1378.46134	3323.49521
	Cu = 120	1467.251045	1752.69708	4274.76471

The result of the plastic shear (or PEEQ) at the point of failure of the strip footing in the present study is illustrated in Fig. 12. Immediately it can be noticed the existence of different areas in the failure zone below the footing which it agrees with the failure mechanism suggested by Georgiadis (2010). PEEQ is the name of the Abaqus parameter for equivalent plastic strain. Essentially, it is a scalar measure of all components of the equivalent plastic strain at each position in the model.

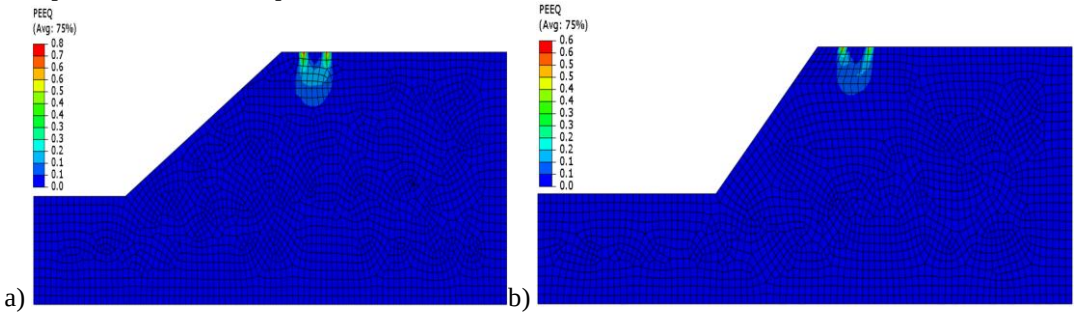

a) b)

Figure 12: Plastic shear distribution at failure (β = 30° y 45°).

5 Conclusions

Each method depends on several factors involved in the estimation of bearing capacity, so it is difficult to identify a single common factor that dominates the ultimate bearing capacity. The conclusions drawn from the present study are:

- The different analytical solutions for the evaluation of the bearing capacity of the shallow foundation on the slope crest have their assumptions and limitations; they were analyzed for cohesive and frictional soils.
- Vesic (1975) which provides the ultimate bearing capacity of a shallow foundation at the top of a slope in cohesive soils is considered for a conservative design compared to the method of Georgiadis (2010), which also takes into account other factors such as the *b/B* ratio but does not take into account D_f/B. For Vesic D_f/B has little influence on its response.
- The method of Hansen (1970) and Sharma and Chen (1995) used for frictional soils differs greatly as the friction angle increases and the slope inclination angle decreases.
- It was found that the numerical results approximate the analytical solutions and is a way to calibrate the numerical model for more advanced simulations.

References

[1] Abaqus (2021) Abaqus Documentation, Dessault Systèmes.
[2] Ahmadi, M.; Asakereh, A. Numerical Analysis of the Bearing Capacity of Strip Footing on Reinforced Soil Slope. International Journal of Engineering Trends and Technology (IJETT), v29 (6), 313-317, 2015.
[3] Baazouzi, M.; Benmeddour, D.; Mabrouki, A.; Mellas, M. 2D Numerical Analysis of Shallow Foundation Rested Near Slope under Inclined Loading. Procedia Engineering; 143, 623-634, 2016.
[4] Graham, J.; Andrews, M.; Shields, D. Stress Characteristics for Shallow footings in Cohesionless Slope. Can. Geotech. J., 25(2), 238-249, 1988.
[5] Georgiadis, K. Undrained bearing capacity of strip footings on slopes. Journal of geotechnical and geoenvironmental engineering, vol. 136, pp. 677-685, 2010.
[6] Hansen, J. A revised and extended formula for bearing capacity. 1970.
[7] Lee, J.; Salgado, R. Estimation of bearing capacity of circular footings on sands based on cone penetration test. Journal of Geotechnical and Geoenvironmental Engineering; 131(4), 442–452, 2005.
[8] Lopez, M. Quevedo, R. Modeling of settlement and bearing capacity of Shallow foundations in overconsolidated clays. Journal of GeoEngineering, vol. 17, No. 1, pp. 001-010, 2022.
[9] Mabrouki, A., Benmeddour, D., Frank, R., Mellas, M. Numerical study of the bearing capacity for two interfering strip footings on sands. Computers and Geotechnics; 37(4), 431–439, 2010.
[10] Meyerhof, G. The ultimate bearing capacity of foundations on slopes. in Proc., 4th Int. Conf. on Soil Mechanics and Foundation Engineering, pp. 384-386, 1957.
[11] Resende, B.; Martin, J.; Asce, M. Formulation of Drucker-Prager Cap Model, I(7), pp. 855–881, 1985.
[12] Sandler, I.; DiMaggio, F.; Baladi, G. A generalized cap model for geological materials. ASCE, GT Div., 102(November), pp. 683–697, 1976.
[13] Saran, S.; Sud, V.; Handa, S. Bearing Capacity of Footings Adjacent to Slopes. Journal Geotech. Engg., ASCE, 115(4), 553–573, 1989.
[14] Sarma, S.; Chen, Y. Bearing Capacity of Strip Footing near Sloping Ground during Earthquake. In Proc. XIth WCEE, Acapulco, Mexico, Paper No. 2078, 1996.
[15] Shiau, J.; Merifield, R.; Lyamin, A.; Sloan, S. Undrained stability of footings on slopes, International Journal of Geomechanics, vol. 11, pp. 381-390, 2011.
[16] Terzaghi, K. Theoretical soil mechanics. Wiley, 1943
[17] Vesic, A. Bearing capacity of shallow foundations. Foundation Engineering. Handbook. ed. H. F. Winterkorn and H. Y. Fang, Van Nostrand Reinhold Co., New York. pp. 121-147, 1975.